

# Ultra-High-Field Targeted Imaging of Focal Cortical Dysplasia: The Intracortical Black Line Sign in Type IIb

 E. Bartolini,  M. Cosottini,  M. Costagli,  C. Barba,  L. Tassi,  R. Spreafico,  R. Garbelli,  L. Biagi,  A. Buccoliero,  F. Giordano, and  R. Guerrini



## ABSTRACT

**BACKGROUND AND PURPOSE:** Conventional MR imaging has limitations in detecting focal cortical dysplasia. We assessed the added value of 7T in patients with histologically proved focal cortical dysplasia to highlight correlations between neuropathology and ultra-high-field imaging.

**MATERIALS AND METHODS:** Between 2013 and 2019, we performed a standardized 7T MR imaging protocol in patients with drug-resistant focal epilepsy. We focused on 12 patients in whom postsurgical histopathology revealed focal cortical dysplasia and explored the diagnostic yield of preoperative 7T versus 1.5/3T MR imaging and the correlations of imaging findings with histopathology. We also assessed the relationship between epilepsy surgery outcome and the completeness of surgical removal of the MR imaging–visible structural abnormality.

**RESULTS:** We observed clear abnormalities in 10/12 patients using 7T versus 9/12 revealed by 1.5/3T MR imaging. In patients with focal cortical dysplasia I, 7T MR imaging did not disclose morphologic abnormalities ( $n=0/2$ ). In patients with focal cortical dysplasia II, 7T uncovered morphologic signs that were not visible on clinical imaging in 1 patient with focal cortical dysplasia IIa ( $n=1/4$ ) and in all those with focal cortical dysplasia IIb ( $n=6/6$ ). T2\*WI provided the highest added value, disclosing a peculiar intracortical hypointense band (black line) in 5/6 patients with focal cortical dysplasia IIb. The complete removal of the black line was associated with good postsurgical outcome ( $n=4/5$ ), while its incomplete removal yielded unsatisfactory results ( $n=1/5$ ).

**CONCLUSIONS:** The high sensitivity of 7T T2\*-weighted images provides an additional tool in defining potential morphologic markers of high epileptogenicity within the dysplastic tissue of focal cortical dysplasia IIb and will likely help to more precisely plan epilepsy surgery and explain surgical failures.

**ABBREVIATIONS:** EEG = electroencephalography; FCD = focal cortical dysplasia; SWAN = susceptibility-weighted angiography


**F**ocal cortical dysplasia (FCD) is among the most common structural brain lesions observed in patients who have undergone an operation for drug-resistant epilepsy,<sup>1</sup> reaching up to 78% of neuropathologic findings in pediatric series.<sup>2,3</sup> The neuropathologic spectrum of FCD includes different cytoarchitectural subtypes.<sup>4</sup>

Abnormal cortical layering, affecting either the radial (FCD type Ia) or tangential organization (FCD type Ib) of the cortex,


characterizes FCD type I. Specific cytologic abnormalities within a disrupted cortical lamination separate FCD type II, into IIa (cortical dyslamination + dysmorphic neurons) and IIb (cortical dyslamination + dysmorphic neurons + balloon cells). In FCD type III, lamination abnormalities are associated with different principal brain lesions, namely hippocampal sclerosis (type IIIa),

This work was supported by Projects 133/11 “Ultra-high field MRI targeted imaging of dysplastic cortical lesions and dysembryoplastic tumors” and “Development and Epilepsy: Strategies for Innovative Research to improve diagnosis, prevention and treatment in children with difficult to treat Epilepsy (DESIRE)” and the European Union Seventh Framework Program FP7/2007–2013, grant agreement 602531.

Please address correspondence to Renzo Guerrini, MD, Neuroscience Department, Meyer Children’s Hospital, University of Florence, Viale Pieraccini 24, 50139 Firenze, Italy; e-mail: r.guerrini@meyer.it

 Indicates open access to non-subscribers at [www.ajnr.org](http://www.ajnr.org)

 Indicates article with supplemental on-line appendix and tables.

 Indicates article with supplemental on-line photos.

<http://dx.doi.org/10.3174/ajnr.A6298>

Received June 20, 2019; accepted after revision September 18.

From the Department of Pediatric Neurology (E.B., C.B., A.B., R. Guerrini), Neurogenetics and Neurobiology Unit and Laboratories, and Pediatric Neurosurgery Unit (F.G.), Children’s Hospital A. Meyer-University of Florence, Florence, Italy; Neurology Unit (E.B.), USL Centro Toscana, Nuovo Ospedale Santo Stefano, Prato, Italy; Department of Translational Research and New Technologies in Medicine and Surgery (M. Cosottini), University of Pisa, Pisa, Italy; IMAGO7 Research Foundation (M. Costagli), Pisa, Italy; Epilepsy Surgery Centre C. Munari (L.T.), Ospedale Niguarda, Milano, Italy; Clinical Epileptology and Experimental Neurophysiology Unit (R.S., R. Garbelli), Fondazione Istituto di Ricovero e Cura a Carattere Scientifico, Istituto Neurologico C. Besta, Milano, Italy; and Istituto Di Ricovero e Cura a Carattere Scientifico Fondazione Stella Maris (L.B., R. Guerrini), Pisa, Italy.

tumors (type IIIb), vascular malformations (type IIIc), or any other principal lesions (FCD type IIIId).<sup>4</sup>

FCD type I is a heterogeneous entity deriving from late postmigrational insults to the developing brain, while FCD type II is a more homogeneous malformation, thought to result from early perturbation of cell proliferation and specification.<sup>5</sup> Activating brain somatic mutations in genes of the mTOR pathway are recognized at increasing rates in FCD IIa and IIb and hemimegalencephaly.<sup>4,6,7</sup> Although type I FCD can, at times, be widespread, involving multiple lobes, neuroimaging may be unrevealing. Otherwise, different combinations of imaging signs of FCD have been described, including blurring of the gray/white matter junction, T2-weighted hyperintensity and T1-weighted hypointensity in the subcortical WM, regional hypoplasia/atrophy,<sup>8,9</sup> and cortical thinning.<sup>8,10</sup>

MR imaging signs associated with FCD type II include cortical thickening, increased T2-weighted signal within the cortex or the underlying WM tapering toward the ventricle (ie, transmantle sign), blurring of the GM/WM junction, T2-weighted hyperintensity, and T1-weighted hypointensity in the subcortical WM.<sup>9,11</sup>

However, none of these signs is completely reliable, and the capability of disclosing regions of cortical dysplasia even at 3T MR imaging is suboptimal, especially for FCD types I and IIa.<sup>9,11-13</sup>

In addition, even in patients with MR imaging positive for structural abnormalities the lesion boundaries often escape proper recognition, limiting the possibility of performing tailored surgical resections that reliably include the whole lesion. Although invasive electroencephalographic (EEG) recordings help to identify the seizure-onset zone, histologic abnormalities can extend beyond the electrographic margin,<sup>14</sup> making it problematic to properly define the epileptogenic zone. Poor delimitation of the lesion by MR imaging represents a major drawback because completeness of the surgical resection is a key element for a favorable seizure outcome after the operation.<sup>15-20</sup> Improving the detection rate of FCD and reliably identifying the malformation boundaries are therefore crucial for optimizing surgical planning.

Ultra-high-field MR imaging offers an enhanced spatial resolution reaching microscopic values due to its high signal-to-noise ratio, allowing the different components within the cortex to be visualized, especially through sequences weighted in T2\* and magnetic susceptibility.<sup>21-23</sup> The 7T MR imaging has the capability of disclosing areas of polymicrogyric cortex in brain regions previously considered normal using 3T MR imaging<sup>24</sup> and of uncovering cryptic regions of cortical dysplasia in patients with MR imaging negative for focal epilepsy.<sup>25</sup> The 7T MR imaging has also proved superior to conventional neuroimaging in disclosing radiologic signs of FCD.<sup>26</sup>

We studied 12 patients with FCD using 7T MR imaging and correlated imaging characteristics with neuropathology findings and postoperative epilepsy outcome.

## MATERIALS AND METHODS

Between 2013 and 2019, we performed a 7T MR imaging protocol of investigation with no sedation in patients with drug-resistant focal epilepsy (8 years of age or older).

We performed a retrospective analysis of a suitable surgical series focusing on 12 of these patients who fulfilled the following

inclusion criteria: 1) clinical and EEG findings suggestive of a focal, single seizure-onset zone; 2) previous preoperative 1.5/3T brain MR imaging performed with an optimized protocol for focal epilepsy, including at least 3D T1-weighted (maximum section thickness, 1 mm), coronal/axial T2-weighted, and FLAIR sequences (maximum section thickness, 3 mm); 3) high-quality preoperative 7T brain MR imaging; 4) ablative brain operation with a histopathologic diagnosis of FCD; and 5) availability of postsurgical 1.5/3T MR imaging.

We sought to explore the structural characteristics of FCD using ultra-high-field MR imaging with respect to the specific histologic subtype and to correlate morphologic data with postoperative epilepsy outcome, as defined by the Engel criteria.<sup>27</sup> The study protocol received approval of the Italian Ministry of Health and the Pediatric Ethics Committee of the Tuscany Region. Written informed consent was obtained from all patients or their representatives.

## MR Imaging Acquisitions

All patients had preliminarily undergone diagnostic 1.5/3T studies with dedicated protocols for focal epilepsy (On-line Appendix).

We performed the 7T brain MR study at the IMAGO7 Foundation, Pisa, Italy, on a Discovery MR 950 MR imaging scanner (GE Healthcare; Chicago, Illinois) equipped with a 2-channel quadrature transmit/32-channel receive head coil (Model NM008-32-7GE-MR950, Nova Medical, Wilmington, Massachusetts).

The research study protocol was developed for the investigation of focal epilepsy and consisted of the following sequences: 3D T1-weighted fast-spoiled gradient recalled or 3D T1-weighted Silent<sup>28</sup> with spatial resolution of  $1 \times 1 \times 1$  mm<sup>3</sup>, 3D magnetization-prepared FLAIR sequence<sup>29</sup> with spatial resolution of  $0.7 \times 0.7 \times 0.7$  mm<sup>3</sup>, 3D susceptibility-weighted angiography (SWAN) with spatial resolution of  $0.328 \times 0.438 \times 1.2$  mm<sup>3</sup>, targeted 3D-SWAN with spatial resolution of  $0.6 \times 0.6 \times 0.6$  mm<sup>3</sup> used to also produce quantitative susceptibility maps (On-line Appendix), 2D T2\*WI targeted dual echo gradient recalled echo and 2D T2-weighted FSE, both with in-plane resolution of  $0.313 \times 0.313$  mm<sup>2</sup> and section thickness of 2 mm, and 2D targeted gray-white matter tissue border enhancement FSE-inversion recovery<sup>30</sup> with in-plane resolution of  $0.5 \times 0.5$  mm<sup>2</sup> and section thickness of 2 mm. We chose the localization of targeted sequences according to the seizure-onset zone, as defined by clinical and EEG findings.

Postsurgical brain MRIs were obtained either on the 1.5T (ACS-NT and Achieva) or 3T (Achieva; Philips Healthcare, Best, the Netherlands) MR imaging systems, with minimum sequence requirements of 3D T1-weighted (maximum section thickness, 1 mm), coronal/axial T2-weighted, and FLAIR sequences (maximum section thickness, 3 mm).

## Brain MR Imaging Analysis and Interpretation

One experienced neuroradiologist and 1 neurologist with expertise in advanced neuroimaging, blinded to the histopathologic diagnosis and to the epilepsy outcome, evaluated both the preoperative 1.5/3T and 7T examinations for signs of FCD (increased

cortical thickness, cortical thinning, abnormal sulcation, regional hypoplasia/atrophy, transmantle sign, blurring of the GM/WM junction, T2-weighted hyperintensity, and T1-weighted hypointensity in subcortical WM). The analysis was performed in a joint session on a dedicated workstation (Advantage Workstation 4.6; GE Healthcare).

To optimize assessment of the extent of surgical resection, we aligned images of the postsurgery clinical MR imaging with those acquired with the 7T system using the FMRIB Linear Image Registration Tool (FLIRT; <http://www.fmrib.ox.ac.uk/fsl/fslwiki/FLIRT>).<sup>31</sup>

### **Surgical Procedure and Histopathologic Assessment**

We planned the surgical resections on the basis of the epileptogenic zone, as defined according to each patient's clinical, imaging, and EEG characteristics.

The histopathologic review of resected brain tissue was performed at Children's Hospital Anna Meyer, Florence, and at the Istituto Neurologico Carlo Besta, Milan, by 3 experienced neuropathologists (On-line Appendix). Histopathologic interpretation was based on the international league against epilepsy (ILAE) classification of focal cortical dysplasia.<sup>4</sup> To explore the histopathologic counterpart of the radiologically defined black line (see below), we relied on macroscopic anatomic landmarks on the surgical specimen, limited to patients who had stereo-EEG recordings (patients 3 and 7), on electrode traces.

### **RESULTS**

Demographic and clinical information of the study population is shown in the On-line Table. Neuropathologic assessment revealed FCD Ib in 2 patients (patients 5 and 6), FCD IIa in 4 (patients 4, 8, 9, and 12), and FCD IIb in 6 (patients 1–3, 7, 10, and 11).

Preoperative 1.5/3T MR imaging revealed abnormal findings in 9/12 (75%) patients. In detail, in the 2 patients with FCD Ib, 1.5/3T MR imaging was unrevealing; in the 4 patients with FCD IIa, there was blurring of the GM/WM junction, which was associated with lobar hypoplasia, abnormal gyral contouring, and, in 1 patient, increased cortical thickness. Patients with FCD IIb had either unrevealing 1.5/3T MR imaging findings (Patient 10) or exhibited variably combined signs of FCD, namely abnormal sulcal/gyral contouring (patients 2, 3, 7, and 11), increased cortical thickness (patients 3, 7, and 11), increased T2-weighted intracortical signal (patients 1, 3, and 7), blurring of the GM/WM junction (patients 1–3 and 11), a T2-weighted hyperintense transmantle sign (patients 1–3, 7, and 11), T2-weighted hyperintensity in the subcortical WM (patients 1–3, 7, and 11), and T1-weighted hypointensity in the subcortical WM (patients 2, 3, 7, and 11).

The 7T MR imaging examination demonstrated clear morphologic or signal abnormalities in 10/12 (83%) patients. In both patients with FCD Ib, we considered 7T MR imaging to be unrevealing, though we observed a nonspecific granular and blurry appearance of the subcortical WM, which was not visible on previous examinations (On-line Fig 1). In all 10 patients with FCD II, the 7T MR imaging examination confirmed the 1.5/3T findings but revealed additional subtle signs in one of the patients with FCD IIa (patient 12) and in all those with FCD IIb (patients

1–3, 7, 10, and 11). The elevated spatial resolution allowed a better visualization of the abnormal gyral contouring in all patients with FCD IIb and in 1 with FCD IIa (patient 12), resolving the anatomic details of a single gyrus, which yielded an apparent increased cortical thickness on conventional imaging due to partial volume effects.

The transmantle sign and the WM signal alterations were clearly defined due to the high 7T SNR in 5/5 patients with such radiologic features. Susceptibility-weighted images revealed an abnormal venous drainage undisclosed by conventional angiogram venography in 1 patient (patient 2) and depicted a peculiar intracortical hypointense band (black line) with high susceptibility on quantitative susceptibility maps in 5/6 patients with FCD IIb (patients 1–3, 7, and 10, whose 1.5/3T T2\*-weighted images were unrevealing) (Figs 1 and 2).

Postsurgical histopathology demonstrated widespread dysmorphic neurons and balloon cells over the cortical regions having such a T2\*WI hypointense band (black line) (patients 1–3, 7, and 10) (On-line Fig 2). On the contrary, dysmorphic neurons and balloon cells spared the cerebral cortex and were atypically limited to subcortical WM in the single patient with FCD IIb who did not exhibit the T2\*WI hypointense black line on 7T imaging (patient 11).

Postsurgical outcome was unsatisfactory in both patients with FCD Ib (patients 5 and 6), while it was favorable in 8/10 (80%) of those with FCD II (Engel class I, patients 1–4, 8–10 and 12). In patients with FCD IIb, by analyzing the coregistration between the 7T examination and the postsurgical MR imaging, we could assess whether the surgical procedure had completely removed the WM/GM blurring ( $n = 3/4$ ), the transmantle sign ( $n = 0/4$ ), the subcortical T2-weighted hyperintense region ( $n = 1/3$ ), and the intracortical black line ( $n = 4/5$ ) (On-line Table 2).

We found that incomplete removal of subcortical regions corresponding to the transmantle sign (patients 1–3) or to T2-weighted hyperintensity (patient 1) did not hamper a favorable epilepsy outcome (ie, Engel class I). Conversely, cortical resections with either incomplete removal of the underlying area of GM/WM blurring seen in FCD IIa ( $n = 1/4$ , patient 8) or of the intracortical T2\*WI black line typical of FCD IIb ( $n = 1/5$ , patient 7) yielded an unfavorable postsurgical outcome (ie, Engel classes II–IV). In patients 3 and 7, we also acquired postoperative 7T scans. In patient 7, who still experienced drug-resistant seizures during follow-up, a residual intracortical hypointense black line persisted next to the surgical crater in the SWAN images of the postoperative 7T scan (Fig 1). Conversely, the black line had completely disappeared in patient 3, who was seizure-free after the operation (Fig 2).

### **DISCUSSION**

In our series of 12 surgically treated patients with histologically proved FCD, 7T MR imaging acquisition yielded positive results in 10 of them, identifying FCD type II in 10/10 exhibiting this histopathologic subtype. From a neuroimaging perspective, the capability of conventional MR imaging to detect signs of cortical dysplasia has been demonstrated to be suboptimal because about half of patients with FCD type I,<sup>9</sup> 10% of those with type IIb,<sup>32</sup> and up to 49% of those with type IIa<sup>11</sup> are reported to exhibit nonspecific MR imaging findings.

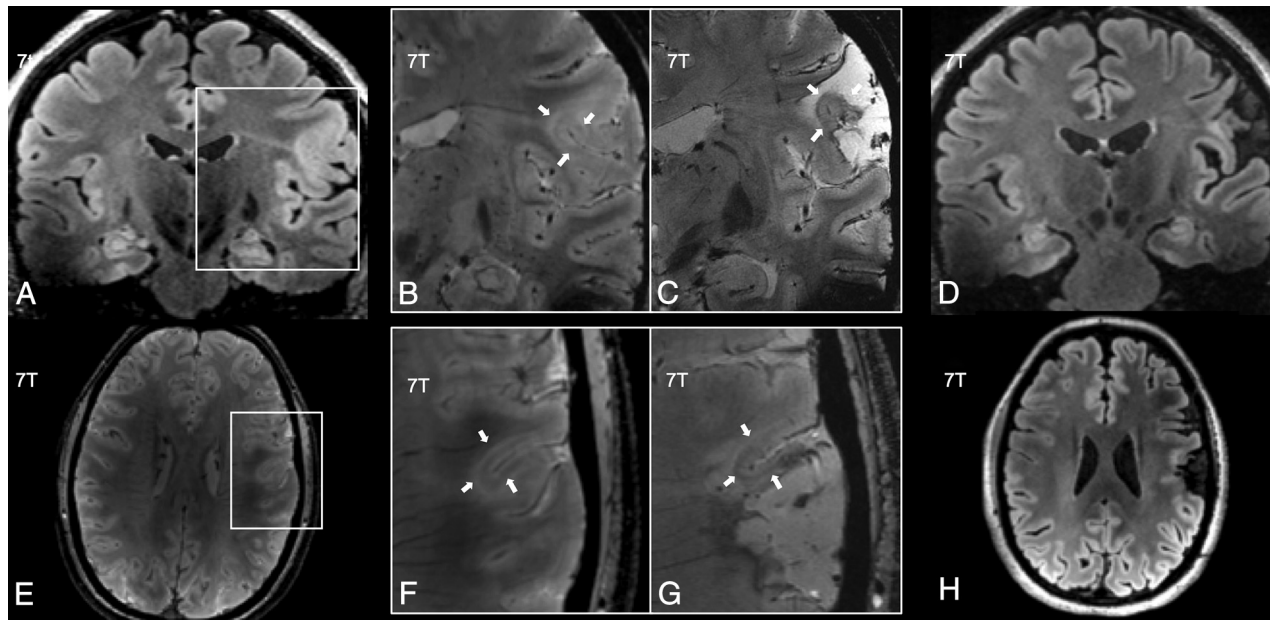


**FIG 1.** A 7T brain imaging of patient 7 (FCD IIb) with unsatisfactory postoperative outcome (Engel class III). A 7T preoperative FLAIR (A), magnified preoperative (B) and postoperative (C) coronal gradient recalled-echo images, postoperative coronal FLAIR (D), preoperative axial SWAN image (E), magnified preoperative (F) and postoperative (G) axial SWAN images, and postoperative axial FLAIR (H). Before the operation, FLAIR images show the transmante sign, while T2\*WI reveals an intracortical hypointense layer (black line) (white arrows in B and F). Postoperative T2\*WI highlights the persistence of the intracortical hypointense layer black line, next to the postsurgical crater (white arrows in C and G). Postoperative FLAIR images (D and H) show that the transmante sign and the white matter hyperintensity were not surgically removed.

As observed in previous studies,<sup>25,26</sup> 7T may uncover structural abnormalities that are not apparent using conventional imaging.

However, in this series, the diagnostic gain was confined to FCD type II, while only minor features could be identified with hindsight in FCD type I (On-line Fig 1).

Ultra-high field imaging revealed with higher resolution the MR imaging signs previously observed by 1.5/3T exams and also detected additional subtle findings in FCD IIb. In particular, we identified a new imaging marker of FCD IIb, consisting of an intracortical band of hypointense signal, visible using SWAN sequences, which we termed “black line,” located in the deep layers beneath seemingly preserved upper cortical layers. We first observed this intracortical signal change in a patient (included here as patient 10) with FCD type IIb, belonging to a clinical series of focal epilepsies studied at 7T,<sup>25</sup> and have now confirmed it in all patients with pathologically proved type IIb FCD (patients 1–3, 7, and 10), except patient 11, who atypically exhibited balloon cells and dysmorphic neurons only in the subcortical WM but not within the cortex.

In a study matching ex vivo 7T imaging with histopathology, T2-weighted imaging disclosed an inhomogeneous intracortical signal intensity in the core of FCD IIb lesions, corresponding to disorganized myelinated fibers and numerous clustered dysmorphic neurons and balloon cells.<sup>33</sup> In view of the similarities our in vivo images have with these ex vivo findings, it is possible that the clustering of abnormal cells and disorganized intracortical fibers of type IIb FCD represent the pathologic substrate of the intracortical black line layer.

Overall, T2\*WI signal decreases with reduced fiber and neuronal cell density, as reported in both the normal and dysplastic cerebral cortex of FCD type I and IIa.<sup>34,35</sup> FCD type IIb features hypomyelination and neuronal rarefaction,<sup>36</sup> yet the contribution

of intracortical dysmorphic neurons and balloon cells in generating the in vivo T2\*WI signal is still unclear. T2\*WI signal intensity might also be modulated by the amount of intracortical iron, but clear evidence of increased microglia<sup>35</sup> or abnormal iron concentration is still lacking.<sup>34</sup> Quantitative histopathology would be essential for a comprehensive understanding of the relationship between tissue microstructure and MR imaging signal changes in FCD subtypes.<sup>37</sup> From a clinical perspective, although our series is too small to draw firm conclusions, we are inclined to consider the black line as sensitive and specific for FCD II since we never observed it in association with other subtypes of dysplasia and in healthy controls (published in part in Cosottini et al<sup>38</sup>).

About 80% of patients with FCD IIb also exhibited the transmante sign, which both conventional and ultra-high-field imaging clearly revealed. This sign is more frequently observed in type IIb FCD<sup>11</sup> and reflects a reduction of myelinated fibers, with high density of balloon cells and reduced oligodendrocytes with abnormal nuclei.<sup>36</sup> Defective myelination is likely the consequence of an exuberant balloon cell proliferation in early proliferation corticogenesis, likewise observed in tuberous sclerosis complex.<sup>39</sup> In 5/6 patients with FCD IIb, 7T imaging also revealed signal changes in the subcortical white matter. In 4 of these patients, all exhibiting both white matter hyperintensity and the intracortical black line (4/6 patients with FCD IIb), T2\*WI bears a resemblance to the flaglike appearance described by Colon et al<sup>26</sup> using 7T in FCD. In a single patient, we also uncovered a venous drainage abnormality (patient 2), which may sometimes be located next to the dysplastic cortex in malformations of cortical development.<sup>40</sup>

To quantify the completeness of surgical excision and correlate it with clinical outcome in patients with FCD IIb, we



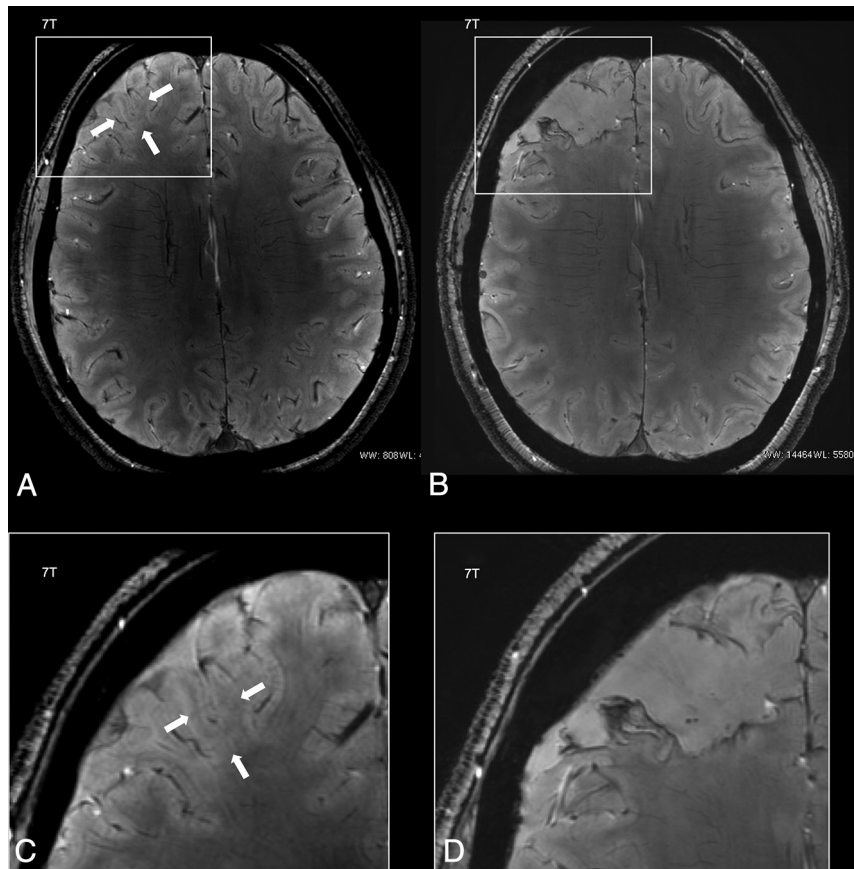


**FIG 2.** A 7T brain imaging of patient 3 (FCD IIb), with favorable postoperative outcome (Engel class I); 7T axial preoperative (A and C) and postoperative (B and D) SWAN images. Preoperative T2\*WI (A) shows an intracortical hypointense layer (black line, white arrows, magnified in C). Postoperative T2\*WI (B, magnified in D) demonstrates the complete removal of the intracortical hypointense layer (black line).

compared the preoperative and postoperative MR imaging. For this purpose, we coregistered ultra-high-field SWAN imaging with preoperative high-resolution anatomic T1-weighted images. Coregistration with postoperative anatomic T1-weighted images was then obtained to establish the relationship between the spatial coordinates of FCD and the postsurgical crater. Rigid coregistration of pre- and postoperative images did not guarantee an optimal comparison in 2/6 patients (patients 2 and 3) because the postresection brain was largely distorted. To obviate this limitation, we used anatomic landmarks to visually assess removed-versus-spared FCD tissue.

We found that in patients with FCD IIb, clinical outcome correlated with the complete removal of the intracortical black line because its complete excision was accompanied by the best post-surgery outcomes (patients 1–3, 10, and 11), while the only patient with incomplete removal still experienced disabling seizures during follow-up (patient 7).

Persistence of the transmantle sign after the operation did not hamper a good seizure outcome (patients 1, 2, and 3), confirming that the demyelinated white matter underlying the dysplastic cortex is not necessarily and directly related to epileptogenesis.<sup>41</sup>

sensitivity of SWAN images at ultra-high-field strengths in detecting the intracortical component of FCD IIb, which we designated as the black line, represents a potential adjunctive tool for characterizing the epileptogenic dysplastic cortex and defining its extent, thereby improving surgical planning and prognostication, and weighting the indications for a re-operation in case of failure. A study specifically addressing the presence of the black line sign on standardized 3T MR imaging would provide further information on the clinical value of such findings in clinical practice.

Disclosures: Renzo Guerrini—RELATED: Grant: European Union, Comments: Projects 133/II “Ultra-high field MRI targeted imaging of dysplastic cortical lesions and dysembryoplastic tumors” and “Development and Epilepsy: Strategies for Innovative Research to improve diagnosis, prevention and treatment in children with difficult to treat Epilepsy (DESIRE)” and European Union Seventh Framework Program FP7/2007–2013, grant agreement 602531.\* \*Money paid to the institution.

## REFERENCES

- Blumcke I, Spreafico R, Haaker G, et al. **Histopathological findings in brain tissue obtained during epilepsy surgery.** *N Engl J Med* 2017;377:1648–56 [CrossRef Medline](#)
- Spencer S, Huh L. **Outcomes of epilepsy surgery in adults and children.** *Lancet Neurol* 2008;7:525–37 [CrossRef Medline](#)

## CONCLUSIONS

We compared conventional brain MR imaging studies performed with different magnet strengths with a standardized 7T MR imaging protocol of investigation. In particular, half of the patients had undergone a preliminary 1.5T scan optimized for epilepsy, and one-fourth of the patients did not have T2\*WI included in conventional MR imaging studies. These limitations hamper a head-to-head comparison with ultra-high-field imaging and limit the generalization of our findings, which should be considered preliminary and exploratory. In addition, we could not focus on a point-by-point correspondence between macroscopic imaging characteristics and histologic findings. Such a drawback could be partially overcome by also studying ex vivo 7T scans of the surgical specimen and including only patients studied by stereo-EEG to use the electrode tracks as landmarks, but technical limitations in coregistration between presurgical and postsurgical brain images are still to be solved. Preoperative investigations of FCD combine electroclinical data, MR imaging, and, in selected patients, [<sup>18</sup>F] FDG-PET and invasive electrophysiologic monitoring.<sup>42</sup> The

3. Palmi A, Holthausen H. **Focal malformations of cortical development: a most relevant etiology of epilepsy in children.** *Handb Clin Neurol* 2013;111:549–65 [CrossRef Medline](#)
4. Blümcke I, Thom M, Aronica E, et al. **The clinicopathologic spectrum of focal cortical dysplasias: a consensus classification proposed by an ad hoc Task Force of the ILAE Diagnostic Methods Commission.** *Epilepsia* 2011;52:158–74 [CrossRef Medline](#)
5. Barkovich AJ, Guerrini R, Kuzniecky RI, et al. **A developmental and genetic classification for malformations of cortical development: update 2012.** *Brain* 2012;135:1348–69 [CrossRef Medline](#)
6. Mirzaa GM, Campbell CD, Solovieff N, et al. **Association of *MTOR* mutations with developmental brain disorders, including megalencephaly, focal cortical dysplasia, and pigmentary mosaicism.** *JAMA Neurol* 2016;73:836–45 [CrossRef Medline](#)
7. Conti V, Pantaleo M, Barba C, et al. **Focal dysplasia of the cerebral cortex and infantile spasms associated with somatic 1q21.1-q44 duplication including the *AKT3* gene: *AKT3* duplication and FCD.** *Clin Genet* 2015;88:241–47 [CrossRef Medline](#)
8. Blümcke I, Pieper T, Pauli E, et al. **A distinct variant of focal cortical dysplasia type I characterised by magnetic resonance imaging and neuropathological examination in children with severe epilepsies.** *Epileptic Disord* 2010;12:172–80 [CrossRef Medline](#)
9. Tassi L, Colombo N, Garbelli R, et al. **Focal cortical dysplasia: neuropathological subtypes, EEG, neuroimaging and surgical outcome.** *Brain* 2002;125:1719–32 [CrossRef Medline](#)
10. Hong S-J, Bernhardt BC, Schrader DS, et al. **Whole-brain MRI phenotyping in dysplasia-related frontal lobe epilepsy.** *Neurology* 2016;86:643–50 [CrossRef Medline](#)
11. Colombo N, Tassi L, Deleo F, et al. **Focal cortical dysplasia type IIa and IIb: MRI aspects in 118 cases proven by histopathology.** *Neuroradiology* 2012;54:1065–77 [CrossRef Medline](#)
12. Colombo N, Salamon N, Raybaud C, et al. **Imaging of malformations of cortical development.** *Epileptic Disord* 2009;11:194–205 [CrossRef Medline](#)
13. Leach JL, Miles L, Henkel DM, et al. **Magnetic resonance imaging abnormalities in the resection region correlate with histopathological type, gliosis extent, and postoperative outcome in pediatric cortical dysplasia.** *J Neurosurg Pediatr* 2014;14:68–80 [CrossRef Medline](#)
14. Cohen-Gadol AA, Özdoğan K, Bronen RA, et al. **Long-term outcome after epilepsy surgery for focal cortical dysplasia.** *J Neurosurg* 2004;101:55–65 [CrossRef Medline](#)
15. Kim DW, Lee SK, Chu K, et al. **Predictors of surgical outcome and pathologic considerations in focal cortical dysplasia.** *Neurology* 2009;72:211–16 [CrossRef Medline](#)
16. Krsek P, Maton B, Jayakar P, et al. **Incomplete resection of focal cortical dysplasia is the main predictor of poor postsurgical outcome.** *Neurology* 2009;72:217–23 [CrossRef Medline](#)
17. Phi JH, Cho BK, Wang KC, et al. **Longitudinal analyses of the surgical outcomes of pediatric epilepsy patients with focal cortical dysplasia.** *J Neurosurg Pediatr* 2010;6:49–56 [CrossRef Medline](#)
18. Chang EF, Potts MB, Keles GE, et al. **Seizure characteristics and control following resection in 332 patients with low-grade gliomas.** *J Neurosurg* 2008;108:227–35 [CrossRef Medline](#)
19. Rowland NC, Englot DJ, Cage TA, et al. **A meta-analysis of predictors of seizure freedom in the surgical management of focal cortical dysplasia.** *J Neurosurg* 2012;116:1035–41 [CrossRef Medline](#)
20. Oluigbo CO, Wang J, Whitehead MT, et al. **The influence of lesion volume, perilesion resection volume, and completeness of resection on seizure outcome after respective epilepsy surgery for cortical dysplasia in children.** *J Neurosurg Pediatr* 2015;15:644–650 [CrossRef Medline](#)
21. Kwan JY, Jeong SY, Gelderen PV, et al. **Iron accumulation in deep cortical layers accounts for MRI signal abnormalities in ALS: correlating 7 Tesla MRI and pathology.** *PLoS One* 2012;7:e35241. [CrossRef Medline](#)
22. Cosottini M, Donatelli G, Costagli M, et al. **High-resolution 7T MR imaging of the motor cortex in amyotrophic lateral sclerosis.** *AJNR Am J Neuroradiol* 2016;37:455–61 [CrossRef Medline](#)
23. Costagli M, Donatelli G, Biagi L, et al. **Magnetic susceptibility in the deep layers of the primary motor cortex in amyotrophic lateral sclerosis.** *Neuroimage Clin* 2016;12:965–69 [CrossRef Medline](#)
24. De Ciantis A, Barkovich AJ, Cosottini M, et al. **Ultra-high field MR imaging in polymicrogyria and epilepsy.** *AJNR Am J Neuroradiol* 2015;36:309–16 [CrossRef Medline](#)
25. De Ciantis A, Barba C, Tassi L, et al. **7T MRI in focal epilepsy with unrevealing conventional field strength imaging.** *Epilepsia* 2016;57:445–54 [CrossRef Medline](#)
26. Colon AJ, van Osch MJ, Buijs M, et al. **Detection superiority of 7 T MRI protocol in patients with epilepsy and suspected focal cortical dysplasia.** *Acta Neurol Belg* 2016;116:259–69 [CrossRef Medline](#)
27. Engel J. **Update on surgical treatment of the epilepsies. Summary of the Second International Palm Desert Conference on the Surgical Treatment of the Epilepsies (1992).** *Neurology* 1993;43:1612–7
28. Costagli M, Symms MR, Angeli L, et al. **Assessment of Silent T1-weighted head imaging at 7 T.** *Eur Radiol* 2016;26:1879–88 [CrossRef Medline](#)
29. Saranathan M, Tourdias T, Kerr AB, et al. **Optimization of magnetization-prepared 3-dimensional fluid attenuated inversion recovery imaging for lesion detection at 7 T.** *Invest Radiol* 2014;49:290–98 [CrossRef Medline](#)
30. Costagli M, Kelley DAC, Symms MR, et al. **Tissue border enhancement by inversion recovery MRI at 7.0 Tesla.** *Neuroradiology* 2014;56:517–23 [CrossRef Medline](#)
31. Jenkinson M, Bannister P, Brady M, et al. **Improved optimization for the robust and accurate linear registration and motion correction of brain images.** *Neuroimage* 2002;17:825–41 [CrossRef Medline](#)
32. Lerner JT, Salamon N, Hauptman JS, et al. **Assessment and surgical outcomes for mild type I and severe type II cortical dysplasia: a critical review and the UCLA experience.** *Epilepsia* 2009;50:1310–35 [CrossRef Medline](#)
33. Zucca I, Milesi G, Medici V, et al. **Type II focal cortical dysplasia: ex vivo 7T magnetic resonance imaging abnormalities and histopathological comparisons.** *Ann Neurol* 2016;79:42–58 [CrossRef Medline](#)
34. Garbelli R, Zucca I, Milesi G, et al. **Combined 7-T MRI and histopathologic study of normal and dysplastic samples from patients with TLE.** *Neurology* 2011;76:1177–85 [CrossRef Medline](#)
35. Reeves C, Tachrount M, Thomas D, et al. **Combined ex vivo 9.4T MRI and quantitative histopathological study in normal and pathological neocortical resections in focal epilepsy.** *Brain Pathol* 2016;26:319–33 [CrossRef Medline](#)
36. Mühlebner A, Coras R, Kobow K, et al. **Neuropathologic measurements in focal cortical dysplasias: validation of the ILAE 2011 classification system and diagnostic implications for MRI.** *Acta Neuropathol* 2012;123:259–72 [CrossRef Medline](#)
37. Adler S, Lorio S, Jacques TS, et al. **Towards in vivo focal cortical dysplasia phenotyping using quantitative MRI.** *Neuroimage Clin* 2017;15:95–105 [CrossRef Medline](#)
38. Cosottini M, Frosini D, Biagi L, et al. **Short-term side-effects of brain MR examination at 7T: a single-centre experience.** *Eur Radiol* 2014;24:1923–28 [CrossRef Medline](#)
39. Prabowo AS, Anink JJ, Lammens M, et al. **Fetal brain lesions in tuberous sclerosis complex: TORC1 activation and inflammation.** *Brain Pathol* 2013;23:45–59 [CrossRef Medline](#)
40. Cui Z, Luan G. **A venous malformation accompanying focal cortical dysplasia resulting in a reorganization of language-eloquent areas.** *J Clin Neurosci* 2011;18:404–06 [CrossRef Medline](#)
41. Wagner J, Urbach H, Niehusmann P, et al. **Focal cortical dysplasia type IIb: completeness of cortical, not subcortical, resection is necessary for seizure freedom.** *Epilepsia* 2011;52:1418–24 [CrossRef Medline](#)
42. Guerrini R, Duchowny M, Jayakar P, et al. **Diagnostic methods and treatment options for focal cortical dysplasia.** *Epilepsia* 2015;56:1669–86 [CrossRef Medline](#)